Journal of Luminescence 132 (2012) 3093–3097

Contents lists available at SciVerse ScienceDirect

Journal of Luminescence

journal homepage: www.elsevier.com/locate/jlumin

100 MeV Si^{8+} ion induced luminescence and thermoluminescence of nanocrystalline $Mg_2SiO_4:Eu^{3+}$

S.C. Prashantha [a,b], B.N. Lakshminarasappa [a,*], Fouran Singh [c]

[a] Department of Physics, Bangalore University, Bangalore 560 056, India
[b] East West Institute of Technology, Magadi road, Bangalore 560 091, India
[c] Inter University Accelerator Center, Aruna Asaf Ali Marg, New Delhi 110 067, India

ARTICLE INFO

Article history:
Received 29 April 2011
Received in revised form
28 February 2012
Accepted 7 March 2012
Available online 28 May 2012

Keywords:
$Mg_2SiO_4:Eu^{3+}$
Phosphor
SHI
Ionoluminescence
Thermoluminescence

ABSTRACT

Nanoparticles of $Mg_2SiO_4:Eu^{3+}$ have been prepared by the solution combustion technique and the grain size estimated by PXRD is found to be in the range 40–50 nm. Ionoluminescence (IL) studies of $Mg_2SiO_4:Eu^{3+}$ pellets bombarded with 100 MeV Si^{8+} ions with fluences in the range 1.124–22.48×10^{12} ions cm^{-2} are carried out at IUAC, New Delhi, India. Five prominent IL bands with peaks at 580 nm, 590 nm, 612 nm, 655 nm and 705 nm are recorded. These characteristic emissions are attributed to the luminescence centers activated by Eu^{3+} cations. It is found that IL intensity decreases rapidly in the beginning. Later on, the intensity decreases slowly with further increase of ion fluence. The reduction in the ionoluminescence intensity with increase of ion fluence might be attributed to degradation of Si–O (ν_3) and Si–O ($2\nu_3$) bonds present on the surface of the sample. The red emission with peak at 612 nm is due to characteristic emission of $^5D_0\rightarrow{}^7F_2$ of the Eu^{3+} cations. Thermoluminescence (TL) studies of $Mg_2SiO_4:Eu^{3+}$ pellets bombarded with 100 MeV Si^{8+} cations with fluences in the range 5×10^{11} ions cm^{-2} to 5×10^{13} ions cm^{-2} are made at RT. Two prominent and well resolved TL glows with peaks at ~220 °C and ~370 °C are observed. It is observed that TL intensity increases with increase of ion fluence. This might be due to creation of new traps during swift heavy ion irradiation.

1. Introduction

Luminescent materials also known as phosphors are mostly in solid form and they are inorganic in nature. The absorption of energy by these materials takes place through host lattice or impurities. In general, the emission originates from impurities present in the host material [1]. Luminescence could be attributed to f–f or f–d transitions of rare earth ions and their intensity would depend on the site symmetry or nature of ligands [2]. Rare earth doped luminescent materials find practical applications such as detectors, tunable LED's CFL, FEDs etc [3–7]. Among the rare earth ions, trivalent europium (Eu^{3+}) has been recognized as an efficient red luminescent phosphor due to its $^5D_0\rightarrow{}^7F_j$ ($j=0$, 1, 2, 3 and 4) transitions [8,9].

Energetic ions have been exploited by researchers in different ways in the field of materials science. The energy of the ion, ion fluence and ion species greatly affects the properties of phosphors. When an energetic ion penetrates a material, it loses energy mainly in two nearly independent processes involving elastic collision with the nuclei, known as 'nuclear energy loss' which dominates at an energy of 1 KeV/amu and inelastic collisions with the atomic electrons, known as 'electronic energy loss' which dominates at an energy of about 1 MeV/amu or more [10].

IL, also known as ion beam induced luminescence (ILBL), is a technique used for materials analysis. An ion beam is used to excite atoms in a target material and the light emitted is analyzed using a fiber optic based detector. Since visible light results from outer shell transitions, it gives information about the nature of chemical bonds in the materials. IBIL is sensitive to the local chemical environment of compounds and trace substitutes and the microstructures of the network [11–15]. IL spectroscopy is a very useful technique for understanding material phenomena such as radiation matter interaction, impurity characterization, local symmetry studies, origin, color and provenance studies of minerals [16]. Recently, IL studies have been reported on various types of minerals, synthetic materials, insulators, semiconductors, thin films etc [17–19].

Magnesium silicate (Mg_2SiO_4), also known as Forsterite, is a member of the Olivine family and possess orthorhombic crystalline structure used at high temperature applications and as an excellent tunable laser. It exhibits low thermal expansion, good chemical stability and excellent insulation properties even at high

* Corresponding author. Tel.: +91 9448116281; fax: +91 80 22961486.
E-mail address: bnlnarasappa@rediffmail.com (B.N. Lakshminarasappa).

0022-2313/$ - see front matter © 2012 Published by Elsevier B.V.
http://dx.doi.org/10.1016/j.jlumin.2012.03.030

temperatures [20,21]. In the present investigation, an attempt is made to study the emission of light caused by heavy ion irradiation in $Mg_2SiO_4:Eu^{3+}$ using IL and TL techniques.

2. Experimental

Nanocrystalline $Mg_2SiO_4:Eu^{3+}$ powder used in the present work is synthesized by the solution combustion method, based on the procedure discussed elsewhere [22]. The synthesized sample is characterized by PXRD (Philips PW 1050/70, CuKα radiation with Ni Filter) and FTIR (Perkin-Elmer spectrometer, Spectrum 1000) techniques. The material is made in the form of pellets of 8 mm diameter and 1 mm thickness using an homemade pelletizer at a pressure of ~100 MPa. The pellets are irradiated at room temperature with 100 MeV Si^{+8} ions for fluences in the range $(1.124–22.48)\times10^{12}$ ions cm^{-2} using 15UD (16 MV Tandem Van-de Graff type electrostatic) pelletron accelerator [23,24] at Inter University Accelerator Center (IUAC), New Delhi, India. The ion beam is scanned over an area of 5 mm^2 using a magnetic scanner at the beam current of 1.5 pnA. One of the unirradiated pellet is used as the pristine sample. Thermoluminescence glow curves of SHI irradiated $Mg_2SiO_4:Eu^{3+}$ are recorded using a TL set up consisting of a small kanthal heating strip, temperature programmer, photomultiplier tube (RCA 931A), and a millivolt meter (Rishcom 100) at a heating rate of 5 °C s^{-1}.

3. Results and discussion

Ionoluminescence spectra of $Mg_2SiO_4:Eu^{3+}$ samples bombarded with 100 MeV Si^{+8} ions with fluences in the range $(1.124–22.480)\times10^{12}$ ions cm^{-2} are shown in Fig. 1(a). Sharp IL emission with peaks at 580 nm, 590 nm, 612 nm, 655 nm and 705 nm are observed and they are attributed to the luminescence centers activated by Eu^{3+} cations [25,26]. The IL intensity depends on ion species, luminescence activators and quenchers. Fig. 1(b) shows the variation of IL intensity with ion fluence. It is observed that the IL intensity decreases rapidly from its initial value and then remains almost constant with increase in ion fluences. The initial intense IL intensity might be due to intrinsic defects present in the sample. The decrease in IL intensity with Si^{+8} ion fluence may be attributed to the amorphization of the material and it may be explained on the basis of the thermal spike model [27]. When the heavy ion strikes the lattice of the material, most of its energy is employed for the creation of an excited electron cloud. The excited material then stabilizes by emitting energy in different forms. There are two important mechanisms suggested. (i) Non-radiative emission of phonons from the lattice. This process would increase the temperature in the crystal and it would lead to amorphization of the crystalline material. (ii) The radiative emission by excited impurity atoms exist in the matrix from their excited level to their ground level. This emission is very sensitive towards the valence state, coordination and distance from the emitting species to the element to which is coordinated. The light emission observed in this way fades with the ion fluence. A proton beam colliding in a crystalline material generates an electron cloud that appears localized in the lattice thus leaving an excited lattice. Different relaxation mechanisms are available to explain the material to return to its ground state, namely non-radiative and radiative emissions. These mechanisms are dependent on irradiation time. Finally, heating of the lattice will thermally quench all the other forms of emission [28].

Also, the reduction in IL intensity with increase of ion fluence might be attributed to degradation of Si–O (ν_3 and $2\nu_3$) bonds present on the surface of the sample and it is confirmed by FTIR studies of pristine and irradiated samples as shown in Fig. 2 and the data obtained are summarized in Table 1. The Si–O (ν_3 and $2\nu_3$) bonds are completely destroyed in ion irradiated samples. The irradiation effect may lead to the restructuring of the surface

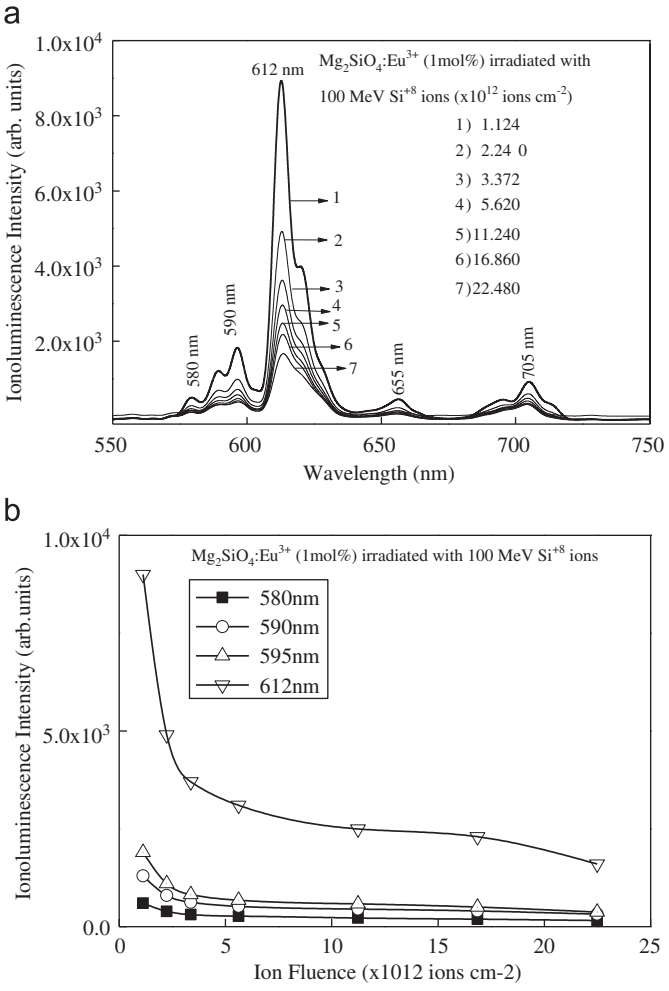

Fig. 1. (a) Ionoluminescence spectra of $Mg_2SiO_4:Eu^{3+}$ irradiated with 100 MeV Si^{+8} heavy ions and (b) variation of IL intensity with ion fluence.

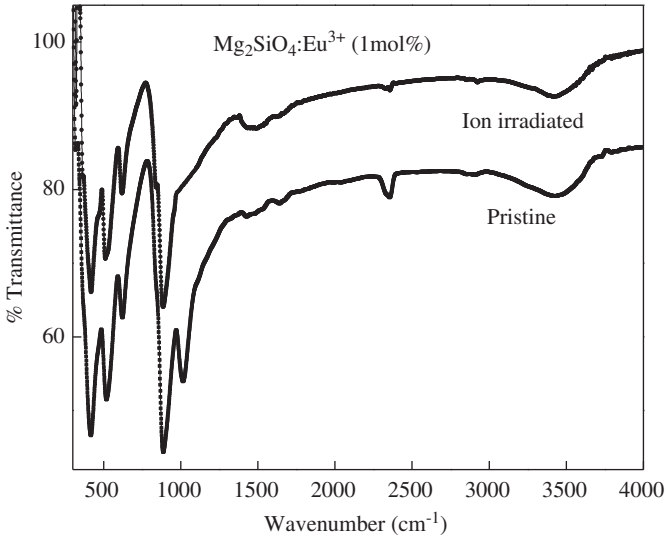

Fig. 2. FT-IR spectra of pristine and SHI (5×10^{13} ions cm^{-2}) irradiated $Mg_2SiO_4:Eu^{3+}$.

Table 1
Assignment of the bond positions of the infrared spectra of pristine and 100 MeV Si^{+8} (5×10^{13} ions cm^{-2}) ion irradiated $Mg_2SiO_4:Eu^{3+}$.

Absorption peak (cm^{-1})	Pristine sample	Irradiated sample
420	MgO_6 octahedral	MgO_6 octahedral
525	Si–O(ν_4)	Si–O(ν_4)
618	Si–O (bending)	Si–O (bending)
680	Mg–O	Mg–O
890	Si–O (stretching)	Si–O (stretching)
1020	Si–O(ν_3)	–
1250	C–H	C–H
1384	NO_3	NO_3
2300	Si–O ($2\nu_3$)	–
3450	–OH (stretching)	–OH (stretching)

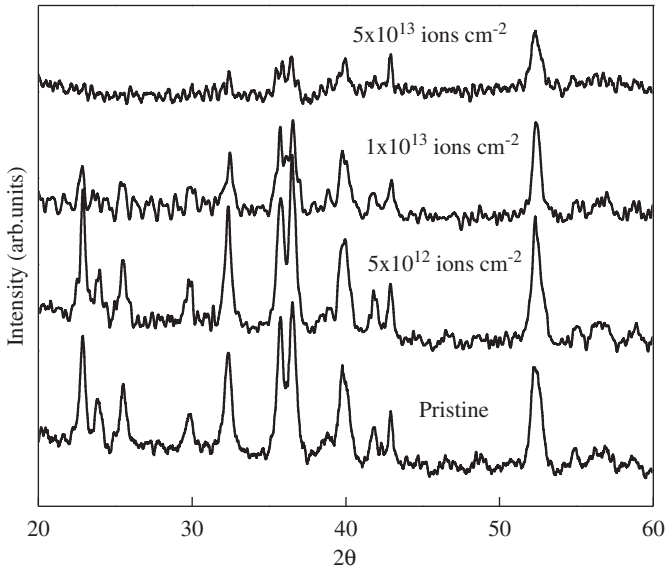

Fig. 3. Glancing angle X-ray diffraction (GXRD) of pristine and SHI irradiated $Mg_2SiO_4:Eu^{3+}$: (a) Pristine, (b) 1×10^{12} (c) 5×10^{12} and (d) 5×10^{13} ions cm^{-2}.

chemical species because of the energy deposited through electronic energy loss during the process of heavy ion irradiation and formation of ion induced defects leading to non-radiative recombination centers at higher fluences [16,29]. It is observed that the OH bond and this stretch bond remains stable with heavy ion irradiation. This confirms that SHI irradiation leads to only surface amorphization instead bulk amorphization of the crystalline sample. The system on the whole remains as radiation resistant [30]. Also, Fig. 3 shows glancing angle X-ray diffraction (GXRD) of a pristine and the samples irradiated with SHI. Broadening and decrease in peak intensity shows occurrence of amorphization due to heavy ion irradiation. Amorphization of crystalline surface leads to surface tracks. These tracks can be related to the defects generated beneath the surface [31].

A series of IL emissions with peaks at 580 nm, 590 nm, 612 nm, 655 nm and 705 nm as shown in Fig. 1(a) may be attributed to the characteristic transitions of Eu^{3+} cations from $^5D_0\rightarrow{}^7F_j$ (j=0,1,2,3 and 4) and is shown in Fig. 4. In particular, emission with peak at 612 nm corresponding to $^5D_0\rightarrow{}^7F_2$ occurs through the forced electric dipole (FED), while the $^5D_0\rightarrow{}^7F_1$ at 590 nm is due to the magnetic dipole transitions. The peak around 612 nm and 590 nm denote that the Eu^{3+} cations occupy the Mg^{2+} sites with C2 or S6 symmetry. These two emissions are of particular interest because they actually represent the local environment of the Eu^{3+} cations. The $^5D_0\rightarrow{}^7F_1$ is due to the

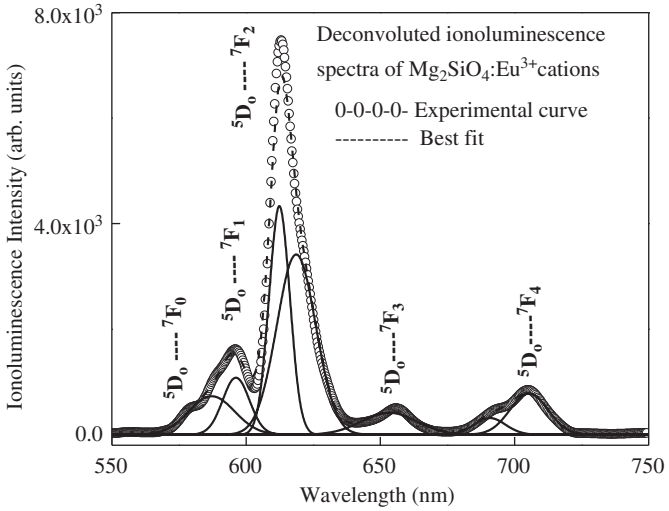

Fig. 4. Deconvoluted ionoluminescence spectra of $Mg_2SiO_4:Eu^{3+}$ irradiated with 100 MeV Si^{+8} heavy ions (22.480×10^{12} ions cm^{-2}).

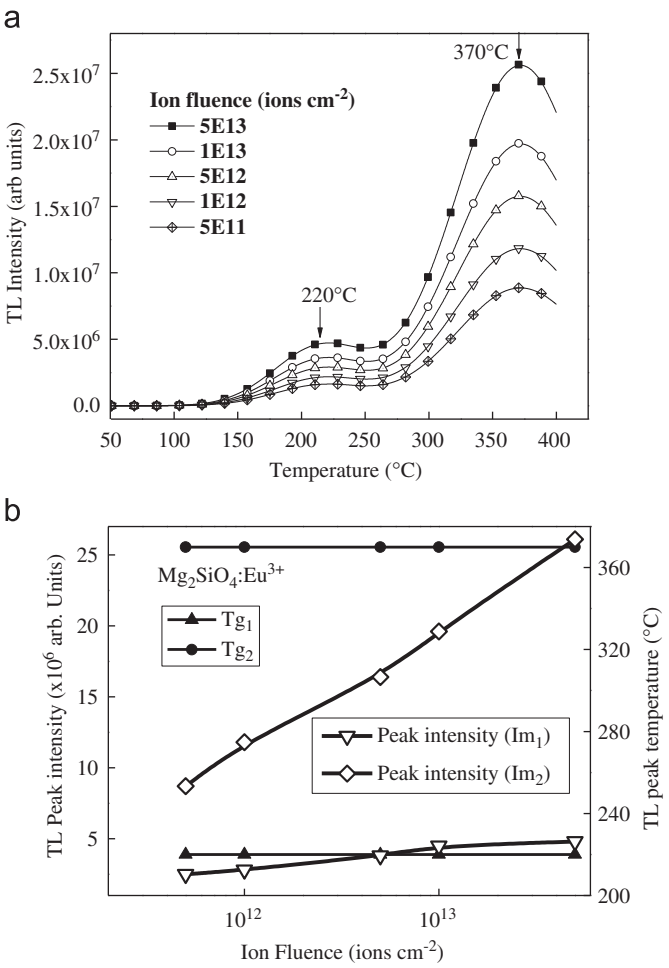

Fig. 5. (a) Thermoluminescence glow curves of SHI irradiated $Mg_2SiO_4:Eu^{3+}$ and (b) variation of TL glow peak intensity and glow peak temperature with ion fluence.

magnetic dipole allowed and its intensity shows variation with the crystal field strength surrounding the Eu^{3+} cations whereas, $^5D_0\rightarrow{}^7F_2$ hypersensitive transition is due to the electric dipole allowed and its intensity is sensitive to the local structure acting

on the Eu^{3+} cation [32–36]. The Eu^{3+} cations enter into the host lattice and replace magnesium ions located on the surface of the nano crystals because of the porosity of Mg_2SiO_4 phosphors. As dopant concentration of Eu^{3+} cations increases, $^5D_0 \rightarrow {}^7F_2$ transition dominates and the emission intensity increases and it may be attributed to the increasing distortion of the local field around the Eu^{3+} cations [37]. It further, results in the luminescence intensity redistribution between the host and the dopant [38]. The host material Mg_2SiO_4 is a member of the olivine family of crystals with orthorhombic crystalline structure in which Mg^{2+} occupies two nonequivalent octahedral sites: one (M1) with inversion symmetry (Ci) and the other (M2) with mirror symmetry (Cs) [39]. In doped Forsterite, Eu^{3+} cations enters into Mg^{2+} lattice site situated at low symmetry sites. Since, ionic radius of Mg^{2+} (0.072 nm) is smaller than Eu^{3+} (0.113 nm), Mg_2SiO_4 host could accommodate only small percentage of impurity ions. Moreover, there is charge imbalance in the host lattice due to doping of trivalent Eu^{3+} cations. When RE^{3+} cations doped into the host, they could probably occupy both sites. Based on this, Eu^{3+} is chosen to study luminescent properties of the material [4,40,41].

Fig. 5(a) shows thermoluminescence glow curves of Mg_2SiO_4:Eu^{3+} irradiated with 100 MeV Si^{+8} ions in the fluence range from 5×10^{11} to 5×10^{13} ions cm^{-2}. Variation of TL peak intensity and glow peak temperature with ion fluence is shown in Fig. 5(b). It is found that TL peak intensity increases with increase of ion fluence. The glow curves clearly show two well resolved and well separated glows with peaks around 220 °C (T_{g1}) and 370 °C (T_{g2}). The peak around 220 °C might be due to recombination of charges released from F^+ centers near Mg^{2+}/Eu^{3+} sites [42] and peak around 370 °C may tentatively attributed to recombination of F center electrons with holes associated with SiO_4 and Mg^{2+} sites. TL glow curves were analyzed by computerized glow curve deconvolution based on Gaussian function using Origin 8.1 software as discussed elsewhere [41,43,44] and shown in Fig. 6 for a fluence of 5×10^{11} ions cm^{-2}. The kinetic parameters were calculated according to the glow curve shape method (modified by Chen) [45,46] and results are tabulated in Table 2. The order of kinetics were estimated by the form factor 'μ_g' also known as symmetry factor $\mu_g = (T_2 - T_m)/(T_2 - T_1) = (\delta/\omega)$, where T_1 and T_2 are the temperatures (from the deconvoluted curves) corresponding to the half of the maximum intensities on either side of the glow peak maximum—T_m [47,48].

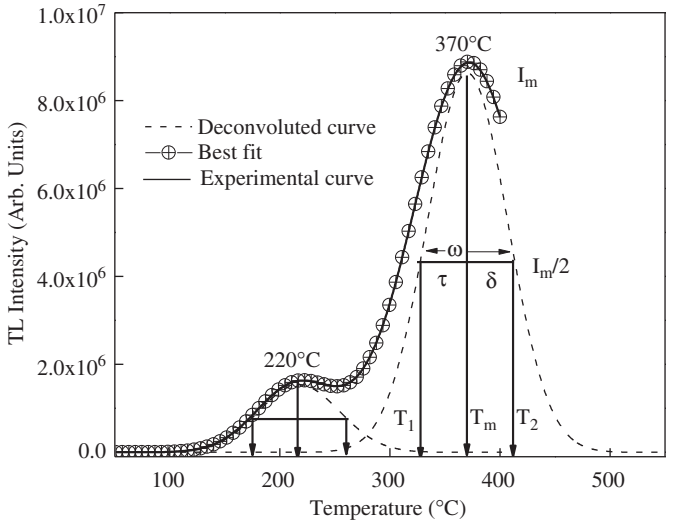

Fig. 6. Deconvoluted (CGCD) thermoluminescence glow curve of SHI irradiated Mg_2SiO_4:Eu^{3+} (5×10^{11} ions cm^{-2}).

4. Conclusions

Mg_2SiO_4:Eu^{3+} nanocrystalline phosphor is prepared in a very short time (< 5 min) using the solution combustion technique. The PXRD pattern showed the presence of alpha phase, orthorhombic structure and the particle size is observed in the nano scale. The phosphor exhibits different emission lines of Eu^{3+} corresponding to $^5D_0 \rightarrow {}^7F_j$ (j=0, 1, 2, 3 and 4) transitions in the range 580–700 nm. The transition centered at 612 nm has found to be hypersensitive in nature which results in a strong and red emission. The decrease in IL intensity might be due to the destruction of the surface chemical species caused by high energy deposited through electronic energy loss during heavy ion irradiation and formation of defects leading to non-radiative recombination centers at higher fluences. The decrease in IL intensity during irradiation might be due to the formation of defects near Mg^+ ions. This causes quenching of the emission feature or blocking the charge migration to the activators. The combination of IL with Particle Induced X-ray Emission (PIXE) may throw a promising light on ion beam analysis for new applications in material science. Ion beam excited luminescence and thermally stimulated luminescence studies of Mg_2SiO_4:Eu^{3+} are reported for the first time from our laboratories. The emitted light shows characteristic features related to the F–F transitions of the RE^{3+} cations in the host material.

Table 2
TL glow peak and kinetic parameters of the glow curve in Eu^{3+}doped Mg_2SiO_4 (μ_g: order of kinetics, E_t: activation energy, n_o: trap density and S: Frequency factor).

Glow peak temperature (T_m; °C)	Ion fluence (ion cm^{-2})	Glow peak parameters				Kinetic parameters		
		δ (°C)	τ (°C)	ω (°C)	μ_g	E_t (eV)	n_o (cm^{-3})	S (s^{-1})
220	5×10^{11}	56	64	120	0.466	0.50	3.46×10^7	7.64×10^3
	1×10^{12}	60	64	124	0.483	0.51	3.11×10^7	10.54×10^3
	5×10^{12}	55	66	121	0.454	0.47	2.94×10^7	3.90×10^3
	1×10^{13}	49	61	110	0.450	0.51	2.04×10^7	9.41×10^3
	5×10^{13}	51	63	114	0.450	0.49	1.94×10^7	6.27×10^3
370	5×10^{11}	66	52	118	0.562	1.00	1.40×10^8	2.40×10^7
	1×10^{12}	63	56	119	0.531	0.91	1.40×10^8	0.40×10^7
	5×10^{12}	57	50	107	0.532	1.04	0.88×10^8	4.17×10^7
	1×10^{13}	59	61	120	0.492	0.81	0.82×10^8	3.70×10^5
	5×10^{13}	63	57	120	0.525	0.89	0.53×10^8	0.24×10^5

References

[1] C.R. Ronda, T. Justel, H. Nikol, J. Alloys Compd. 275 (1998) 669.
[2] Y. Inaguma, T.T. Suchiya, T. Katsumata, J. Solid State Chem. 180 (2007) 1678.
[3] B. Yan, X.Q. Su, Opt. Mater. 29 (2007) 547.
[4] I.M. Nagpure, Subhajit Saha, S.J. Dhoble, J. Lumin. 129 (2009) 898.
[5] M. Salis, J. Lumin. 104 (2003) 17.
[6] J. Zhong, H. Liang, B. Han, X.Q. Su, T. Tao, Chem. Phys. Lett. 453 (2008) 192.
[7] Z.H. Zhang, Y.H. Wang, Y. Hao, W.J. Liu, J. Alloys Compd. 433 (2007) 612.
[8] I. Omkaram, B. Venugopl Rao, Buddudu, J. Alloys Compd. 474 (2009) 565.
[9] H.M. Yang, J.X. Shi, M.L. Gong, J. Alloys Compd. (2006) 213.
[10] D. Kanjilal, Curr. Sci. 80 (2001) 1560.
[11] James R. Huddle, Patrick G. Grant, Alexender R. Ludington, Robert L. Forster, NIM-B 261 (2007) 475.
[12] A. Quaranta, J. Saloman, J.C. Dran, M. Tonezzer, G. Della Mea, NIM-B 254 (2007) 289.
[13] A.A. Bettiol, D.N. Jamieson, S. Prawer, M.G. Allen, NIM-B 85 (1994) 610.
[14] A.A. Bettiol, D.N. Jamieson, S. Prawer, M.G. Allen, NIM-B 85 (1994) 775.
[15] N.P.O. Homman, C. Yang, K.G. Malmqvist, NIM-A 352 (1994) 610.
[16] H. Nagabhushana, B. Umesh, B.M. Nagabhushana, B.N. Lakshminarasappa, F. Singh, R.P.S. Chakradhar, Philos. Mag. 89 (2009) 995.
[17] C. Yang, K.G. Malmqvist, M. Elfman, NIM-B 130 (1997) 746.
[18] J. Zuk, R. Kuduk, M. Kulik, J. Lumin. 57 (1993) 57.
[19] R.J. Brooks, D.E. Hole, P.D. Townsend, NIM-B 190 (2002) 709.
[20] Matthew B.D. Mitchell, David Jackson, Peter F. James, J. Sol–Gel. Sci. Technol. 13 (1998) 359.
[21] M.T. Tsai, Mater. Res. Bull. 37 (2002) 2213.
[22] J.J. Kingsley, K. Suresh, K.C. Patel, J. Mater. Sci. 25 (1990) 1305.
[23] D. Kanjilal, S. Chopra, M.M. Narayanan, I.S. Iyer, V. Jha, S.K. Datta, NIM-A 328 (1993) 97.
[24] H. Nagabhushana, B.N. Lakshminarasappa, F. Singh, D.K. Avasthi, NIM-B 211 (2003) 545.
[25] E. Alves, C. Marques, N. Franco, L.C. Alves, M. Peres, M.J. Soares, T. Monteiro, NIM-B 268 (2010) 3137.
[26] H. Calvo del Castillo, J.L. Ruvalcaba, M. Bettinelli, A. Speghini, M. Barboza Flores, T. Calderón, D. Jaque, J.García Solé, J. Lumin. 128 (2008) 735.
[27] L.H. Abu Hassan, P.D. Townsend, NIM-B 32 (1988) 293.
[28] C. Trautmann, M. Toulemonde, J.M. Costantini, J.J. Grob, K. Schwartz, Phys. Rev. B 62 (2000) 13.
[29] H. Nagabhushana, S.C. Prashantha, B.N. Lakshminarasappa, Fouran Singh, J. Lumin. 128 (2008) 7.
[30] T. Mohanty, N.C. Mishra, F. Singh, U. Tiwari, D. Kanjilal, NIM-B 212 (2003) 179.
[31] G. Szeenes, NIM-B 191 (2002) 27.
[32] Shengping Mao, Qun Liu, Meng Gu, Dali Mao, Chengkang Chang, J. Alloys Compd. 465 (2008) 367.
[33] J. Trojan Piegza, E. Zych, D. Hreniak, W. Strek, L. Kepenski, J. Phys.: Condens. Matter 16 (2004) 6983.
[34] G. Concas, G. Spano, E. Zych, T. Trojan, J. Phys.: Condens. Matter 17 (2005) 2597.
[35] R. Krsmanovi, O.I. Lebedev, A. Speghini, M. Bettinelli, S. Pollizzi, Van Tendello, Nanotechnology 17 (2006) 2805.
[36] Xiang Ying Chen, Chao Ma, Zhong Jie Zhang, Xiao Xuan Li, Microporous Mesoporous Mater. 123 (2009) 202.
[37] Nguyen Vu, Tran kim Anh, Gyu-chul Yi, W. Trek, J. Lumin. 122 (2007) 776.
[38] Oleg Viagin, Andrey Masalov, Irina Ganina, Yuriy Malyukin, Opt. Mater. 31 (2009) 1808.
[39] Hongmei Yang, Jianxin Shi, Menglian Gong, K.W. Cheah, J. Lumin. 118 (2006) 257.
[40] B.N. Lakshminarasappa, S.C. Prashantha, Fouran Singh, Curr. Appl. Phys. 11 (2011) 1274.
[41] S.C. Prashantha, B.N. Lakshminarasappa, B.M. Nagabhushana, J. Alloys Compd. 509 (2011) 10185.
[42] Vijay Singh, T.K. Gundu Rao, Jun-Jie Zhu, J. Lumin. 126 (2007) 1.
[43] C. Furetta, G. Kittis, C.H. Kuo, NIM-B 160 (2000) 65.
[44] Ankush Vij, S.P. Lochab, Surendar Singh, Ravi Kumar, Nafa Singh, J. Alloys Compd. 486 (2009) 554.
[45] N. Suriyamurthy, B.S. Panigrahi., J. Lumin. 128 (2008) 1809.
[46] R. Chen, J. Electrochem. Soc. 116 (1969) 1254.
[47] G. Kittis, J.M.G. Ros, J.W.N. Tuyn., J. Phys. D: Appl. Phys. 31 (1998) 2636.
[48] Q. Fei, C.K. Chang, D.L. Mao, J. Alloys Compd. 350 (2005) 133.